Distance Estimates from Paramagnetic Enhancements of Nuclear Relaxation in Linear and Flexible Model Peptides

Jaison Jacob, Brian Baker, Robert G. Bryant, and David S. Cafiso

From the Department of Chemistry and Biophysics Program, University of Virginia, Charlottesville, Virginia 22901

ABSTRACT The distance dependence of electron–nuclear dipole–dipole coupling was tested using a series of poly-L-proline based peptides of different length. The poly-proline based peptides were synthesized with a nitroxide spin label on the N-terminus and a tryptophan on the C-terminus, and paramagnetic enhancements of nuclear spin-lattice relaxation rates were measured for the aromatic protons on the tryptophan as a function of the number of proline spacers in the sequence. As expected, paramagnetic enhancements decrease with distance, but the distances deduced from the NMR relaxation rates were shorter than expected for every peptide studied compared to a rigid linear poly-L-proline type II helix structure. Calculations of cross-relaxation rates indicate that this difference is not the result of spin-diffusion or the creation of a spin-temperature gradient in the proton spins caused by the nitroxide. Molecular dynamics simulations were used to estimate dynamically averaged value of $\langle r^{-3}\rangle^2$. These weighted average distances were close to the experimentally determined distances, and suggest that molecular motion may account for differences between the rigid linear models and the distances implied by the NMR relaxation data. A poly-L-prolone peptide synthesized with a central glycine hinge showed dramatic relaxation rate enhancements compared to the peptide of the same length lacking the hinge. Molecular dynamics simulations for the hinged peptide support the notion that the NMR data is a representation of the weighted average distance, which in this case is much shorter than that expected for an extended conformation. These results demonstrate that intermoment distances based on NMR relaxation rates provide a sensitive indicator of intramolecular motions.

INTRODUCTION

Biomolecular structures obtained from NMR data are typically generated from a relatively large number of short-range distance constraints. Because they are short-range, these distances are not strongly influenced by macromolecular dynamics. Relatively large distances may be deduced from paramagnetic enhancements of nuclear relaxation (Fesik et al., 1991; Lee et al., 1986; Rosevear et al., 1984; Schmidt and Kuntz, 1984; Sternlicht and Wheeler, 1967). Although relatively few long-range distances can, in principle, define a structure, they are rarely used in standard structure determinations. One difficulty with long-distance measurements is their sensitivity to flexibility or internal dynamics of the macromolecule. This problem also presents an opportunity in that long distances and discrepancies with rigid models of the molecule may be useful measures of molecular flexibility. For example, in the peptide, alamethicin, long-range distances deduced from paramagnetic enhancements of nuclear spin relaxation rates are quite different from those predicted from models derived from x-ray crystallography. These paramagnetic enhancements clearly indicate that the peptide spends a fraction of its time in a bent configuration (North et al., 1994).

In the vicinity of an unpaired electron, the nuclear spin-lattice and spin-spin relaxation rates are dominated by the electron–nuclear dipole–dipole interaction because the electron magnetic dipole moment is large. For protons, the effect of an electron on the nuclear spin-lattice relaxation rate can be easily detected at distances beyond 20 Å. The theory governing the paramagnetic enhancement of nuclear relaxation has been described by Solomon and Bloombergen (Bloombergen et al.; 1948, Solomon, 1955), and, like others (Stryer, 1978; Stryer and Haugland, 1967), this dipole–dipole coupling is proportional to the inverse sixth power of the distance between the electron center and the nucleus.

Here, following an approach taken by Haugland and Stryer, we report an experimental study of the distance dependence of paramagnetic enhancements of nuclear relaxation. Shown in Figure 1 *A* is a rigid poly-L-proline type II helix where a nitroxide is attached to the N-terminus and a tryptophan residue is attached at the C-terminus. Poly-L-proline peptides of different lengths were used to separate the spin-label and tryptophan protons by different lengths to investigate the distance dependence of paramagnetic enhancements in a simple model system known to work well in the fluorescence case. We find that paramagnetic enhancements underestimate the distances based on the rigid model in every case and that the likely source of the discrepancy is a decrease in the effective intermoment distances as a result of intramolecular motional averaging. To test the importance of dynamics, a poly-proline type II helix containing a glycine hinge (Figure 1 *B*) was also studied and

Received for publication 30 November 1998 and in final form 28 April 1999.

Address correspondence and reprint requests to either Robert Bryant or David Cafiso at the Department of Chemistry, University of Virginia, Charlottesville, VA 22901.

Dr. Jacob's present address is National Institute of Dental Research, NIH, Bethesda, MD 20892.

Dr. Baker's present address is La Jolla Pharmaceutical Company, 6455 Nancy Ridge Drive, San Diego, CA 92121.

0006-3495/99/08/1086/07 $2.00

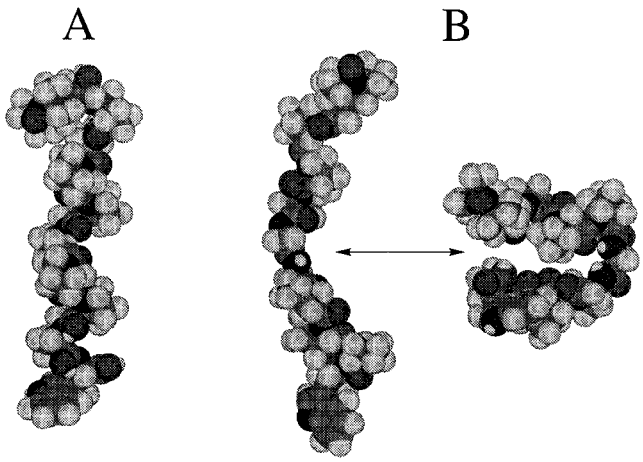

FIGURE 1 (*A*) A model drawing of a poly-L-proline type II helix made of 8 prolines with a proxyl-nitroxide attached to the N-terminus and a tyrptophan residue attached at the C-terminus (P_8W, see Methods). (*B*) A model drawing of a poly-L-proline type II helix having six prolines and two glycines ($P_3G_2P_3W$, see Methods). The two glycines act as a flexible hinge so that the distance between the spin label and indole ring protons of tryptophan vary dramatically as a function of the conformation of the hinge. The structures shown were taken from a 100-ps molecular dynamics simulation of this peptide.

demonstrates that the distances measured from long-range paramagnetic enhancements provide nearly a dynamically averaged distance that approximates a distance of closest approach in highly flexible systems. These results are discussed and they suggest that these long-range distance measurements can provide a sensitive probe of conformational dynamics in macromolecules.

EXPERIMENTAL PROCEDURES

Materials

A series of ten peptides, five spin-labeled and five unlabeled, shown in Table 1 were synthesized. Fmoc-protected aminoacids and 2-chlorotrityl chloride resin were obtained from Novabiochem (San Diego, CA). 1-Hydroxy-benzotriazole hydrate (HOBT), 1,3-diisopropyl-carbodiimide (DIPCDI), and 3-carboxy-proxyl were obtained from Aldrich (Milwaukee, WI). S2 was synthesized by the University of Virginia Biomolecular Research Facility (Charlottesville, VA). The remaining peptides were synthesized as outlined below. D_2O was purchased from Cambridge Isotopes (Andover, MA).

TABLE 1 Peptide sequences used in the study

S1	Pro-Pro-Pro-Pro-Pro-Pro-Trp-OH
S1SL	Proxyl-Pro-Pro-Pro-Pro-Pro-Pro-Trp-OH
S2	Pro-Pro-Pro-Pro-Pro-Pro-Pro-Trp-OH
S2SL	Proxyl-Pro-Pro-Pro-Pro-Pro-Pro-Pro-Trp-OH
S3	Pro-Pro-Pro-Pro-Pro-Pro-Pro-Pro-Trp-OH
S3SL	Proxyl-Pro-Pro-Pro-Pro-Pro-Pro-Pro-Pro-Trp-OH
H1	Pro-Pro-Pro-Gly-Gly-Pro-Pro-Pro-Trp-OH
H1SL	Proxyl-Pro-Pro-Pro-Gly-Gly-Pro-Pro-Pro-Trp-OH
H2	Ace*-Cys-Pro-Pro-Pro-Gly-Gly-Pro-Pro-Pro-Ala*-NH2
H2SL	Ace*-Cys(Proxyl)-Pro-Pro-Pro-Gly-Gly-Pro-Pro-Pro-Ala*-NH2

*Represents a ^{13}C-labeled carbonyl carbon.

Peptide synthesis

Peptides were synthesized using Fmoc chemistry (Stewart and Young, 1984) on 2-chlorotrityl chloride resin, which had been swollen in methanol for 20 min. The Trp residue was attached first by adding 0.6 equivalents of Fmoc-Trp in 10 mL dichloromethane per gram of resin and 4.2 equivalents of diisopropylethylamine with agitatation for 1 h. Deprotection of the Fmoc group was achieved using 20% piperidine. For peptide elongation, Fmoc-protected amino acids, which were activated for 2 min using HOBT and DIPCDI, were added, and the coupling was monitored with bromophenol blue. After the coupling of the last amino acid residue the peptide was spin-labeled. To accomplish this, 3-carboxy-proxyl was activated using HOBT and DIPCDI as before and added to the polypeptide chain while it was still on the resin. To prevent reduction of the spin label during cleavage a low-acid cleavage, mixture containing 1:1:8 acetic acid:trifluoroethanol: dichloromethane was used. The time for the cleavage was 30 min and the peptides were precipitated in cold ether. For purification, an aqueous solution was applied to a semipreparative Vydac reverse phase C18 HPLC column. S1, S1SL, and S3 were eluted using an isopropanol-water gradient; H1, S2SL, and S3SL were eluted using isopropanol with 0.05% triflouroacetic acid-water gradient; S2 was purified using acetonitrile-water gradient and H1SL was purified using acetonitrile-water gradient each with 0.1% triflouroacetic acid. The molecular weights of all the peptides were confirmed using mass spectrometry.

To determine whether the peptides listed in Table 1 assumed a proline type II helix, the circular dichroism spectrum of each peptide was taken in D_20 at a concentration of about 50 μM peptide on a Jasco J-720 spectrometer scanning from 190–250 nm with a 2-nm bandwidth and a scan speed of 50 nm per minute. All the circular dichroism spectra were similar and indicated the presence of one prominent negative band with a minimum at 205 nm, which is indicative of a poly-proline type II helix (Isied and Vassilian, 1984).

NMR spectroscopy

NMR spectra were recorded from D_2O solutions in all cases. For NMR spectroscopy the appropriate amount of peptides were dissolved in D_2O. ^1H NMR spectra were obtained using a Varian UnityPlus 500 spectrometer. Spin-lattice relaxation times were collected using the inversion-recovery sequence, 180-τ-90-acquisition with presaturation of the remaining solvent peak. A typical ^1H T_1 measurement consisted of 13–15 data sets collected for τ values between 10 μs and 10 s. A 7-s relaxation delay was used between scans. For each data set, 16,000 points were collected over a 5000-Hz sweep width. Spectra of unlabeled peptides were taken at a concentration of approximately 3 mM and spin-labeled peptides were taken at a series of concentrations ranging from 3 to 0.3 mM. ^{13}C relaxation measurements were made on a Varian Unity Inova 300 spectrometer using the inversion-recovery sequence without solvent saturation with a sweep width of 3000 Hz. Spectra of unlabeled peptides (^{13}C labeled peptide without the nitroxide) were taken at a concentration of 10 mM, and spin-labeled peptides were taken at a series of concentrations ranging between 10 and 2 mM. The average of three separate T_1 experiments was used to calculate the intermoment distances.

Estimating ^1H-nitroxide distances

The paramagnetic enhancement factor of the nuclear spin-lattice relaxation rate, R_1^{enh} was calculated from

$$R_1^{enh} = R_1^{para} - R_1^{dia}, \quad (1)$$

where, R_1^{dia} is the relaxation rate for the unlabeled peptide and R_1^{para} is relaxation rate of the labeled peptide at infinite dilution obtained by extrapolation of the relaxation rate to zero concentration. The distance, T_1, between the nitroxide and the observed proton, was obtained using the

simplified Solomon–Bloembergen equation,

$$r = C\left\{\left(\frac{3\tau_c}{1+\omega_I^2\tau_c^2}+\frac{7\tau_c}{1+\omega_S^2\tau_c^2}\right)\Big/R_1^{enh}\right\}^{1/6}, \quad (2)$$

where, C is a constant having a value of 540 and 341 Å for ^{1}H and ^{13}C, respectively, and ω_I and ω_S are the nuclear and electron Larmor frequencies (Krugh, 1976). This expression is generally valid for spin labels where the electron relaxation times are long relative to the correlation time, τ_c. The correlation times for the reorientation of the electron–nuclear vector are problematic but were estimated using (Cavanagh et al., 1996)

$$\tau_c = \frac{4\pi\eta r_H^3}{3k_BT}, \quad (3)$$

where r_H is the hydrodynamic radius given by

$$r_H = \left[\frac{3VM}{4\pi N}\right]^{1/3} + r_w.$$

Here, r_W is a correction sometimes blamed on solvation, η is the solvent viscosity, T is the temperature, k_B is the Bolzmann constant, V is the specific volume of the peptide, which is 0.73 cm^3 gm^{-1}, M is the molecular weight and N is Avagadro's number. This choice of model for τ_c presumes that high-frequency motions in the picosecond time scale are of limited amplitude. Nevertheless, because the estimated distance depends upon the sixth root of the correlation time, the distances obtained from Eq. 2 will be relatively insensitive to a modest error in the value of τ_c.

Dynamics simulations

Molecular models for the proline peptides were assembled using InsightII (MSI, Scranton, CA), and molecular dynamics simulations were carried out using Discover95 (MSI, Scranton, CA) through the InsightII interface on a Silicon Graphics R4000 Indigo computer (SGI, Mountain View, CA). The simulation used a constant valence force field with a 1-fs step size and a continuous dielectric of 82. The history of the molecule was saved at every ps interval for analysis of the trajectories. The trajectories from the simulations were analyzed using Decipher (MSI, Scranton, CA), and the weighted distances were calculated by analyzing the output file from Decipher using MATLAB *5.1.0* (The Math Works, Inc., Natick, MA) running on a University of Virginia RS6000 computer.

Relaxation calculations

For a system with N interacting spins, the rate of change of magnetization toward its equilibrium value is given by the first-order differential equation,

$$\frac{dM_z^i}{dt} = -\rho_i M_z^i(t) - \sum_{k\neq i}\sigma_{ik}M_z^k(t), \quad (4)$$

where ρ_i are the direct relaxation rate constants and σ_{ik} are the cross-relaxation rate constants. For a system undergoing isotropic Brownian motion, the quantities ρ_i and σ_{ik} in Eq. 4 are given by

$$\rho_i = \sum_{i\neq k}\rho_{ik},$$

$$\rho_{ik} = \left(\frac{\mu_0}{4\pi}\right)^2\frac{\gamma_i^2\gamma_k^2\hbar^2}{r_{ik}^2}\left[\tau_c+\frac{3\tau_c}{1+\omega_i^2\tau_c^2}+\frac{6\tau_c}{1+4\omega_k^2\tau_c^2}\right],$$

$$\sigma_{ik} = \left(\frac{\mu_0}{4\pi}\right)^2\frac{\gamma_i^2\gamma_k^2\hbar^2}{r_{ik}^2}\left[-\tau_c+\frac{6\tau_c}{1+4\omega_i^2\tau_c^2}\right],$$

where τ_c is the rotational correlation time of the molecule, γ_i and γ_k are the gyromagnetic ratios of the interacting spins, μ_0 is the permeability of free space, and r_{ik} is the intermoment distance. This system of first-order homogeneous linear differential equations can be written in the matrix form as

$$\frac{dM}{dt} = -\Gamma M. \quad (5)$$

The solutions for this system were obtained using the standard routines in MATLAB (The Math Works, Inc., Natick, MA).

RESULTS

Shown in Fig. 2 is the ^{1}H NMR spectrum of the peptide S3 in D_2O. The aromatic residue at the C-terminus provides several resonances that are clearly resolved from the backbone and side chain resonances in the one-dimensional spectrum. Shown in Fig. 3 are the results of the inversion-recovery experiment for the indole protons 4 and 7 on the tryptophan sidechain of peptide H1. As expected, the proton spectrum of the spin-labeled peptide 1HSL exhibits both increased linewidths and enhanced relaxation rates when compared to the spectra obtained from the unlabeled peptide ^{1}H. The magnetization recovery for protons associated with both the labeled and unlabeled peptides were exponential within experimental error.

In solution, nuclear relaxation that is promoted by a spin label can result from both intramolecular and intermolecular contributions; however, the Solomon–Bloembergen equation (Eq. 2) assumes that the interaction is entirely a result of the intramolecular interaction between an electron and a

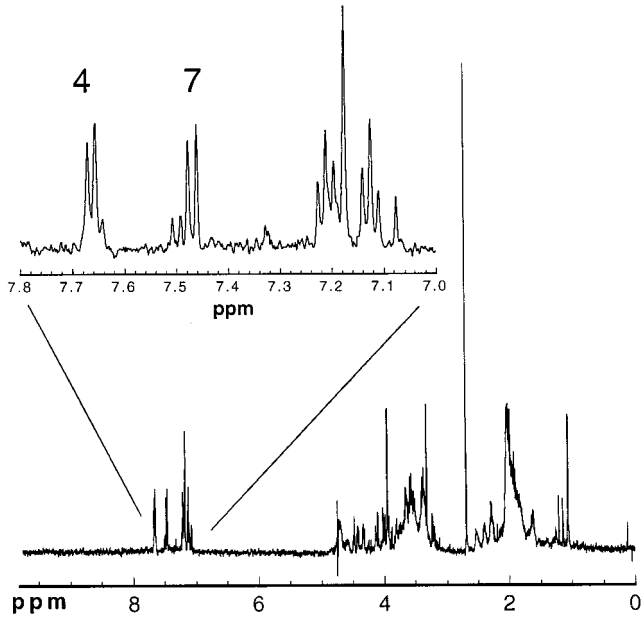

FIGURE 2 ^{1}H NMR spectrum of S3, a poly-L-proline type II helix in aqueous solution. The aromatic resonances from the typtophan indole ring are well-resolved and shifted down field from the other side-chain and backbone protons in the peptide. The expansion between 7.7 and 7.1 ppm shows the indole protons at positions 4 and 7.

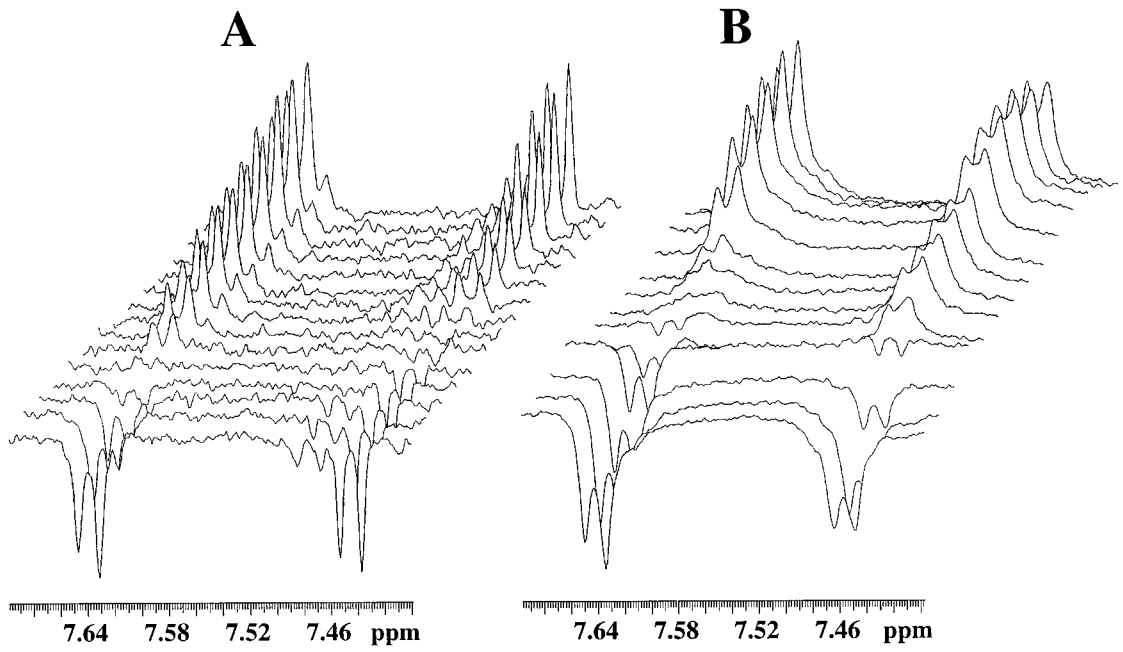

FIGURE 3 ^{1}H NMR spectra in D_2O showing the magnetization of the protons at positions 4 and 7 of the indole ring in tryptophan as measured using the inversion-recovery sequence, π-τ-π/2-acq, as a function of τ. (*A*) Spectra for H1 (see Table 1) where τ has values of 1 μs, 100, 400, and 800 ms, 1.2, 1.6, 2, 2.4, 2.8, 3.2, 3.6, 4, 9, and 12 s (*bottom to top*). (*B*) Spectra for H1SL where τ has values of 1 and 100 μs, 50, 100, 250, 300, 350, 400, 600, and 800 ms, 1, 2, and 4 s.

proton. To obtain the intramolecular paramagnetic contribution to the proton relaxation rate, the relaxation rate of the spin-labeled peptide was determined as a function of peptide concentration. Shown in Fig. 4 are plots of the relaxation rates of the spin-labeled peptides, R_1^{SL}, as a function of peptide concentration for S1SL, S2SL, S3SL, and H1SL. The relaxation rate is a linear function of labeled peptide concentration, which demonstrates that intermolecular contributions to relaxation, which are modulated by translational diffusive motions, may be important. The intramolecular contribution may be isolated by extrapolation to infinite dilution.

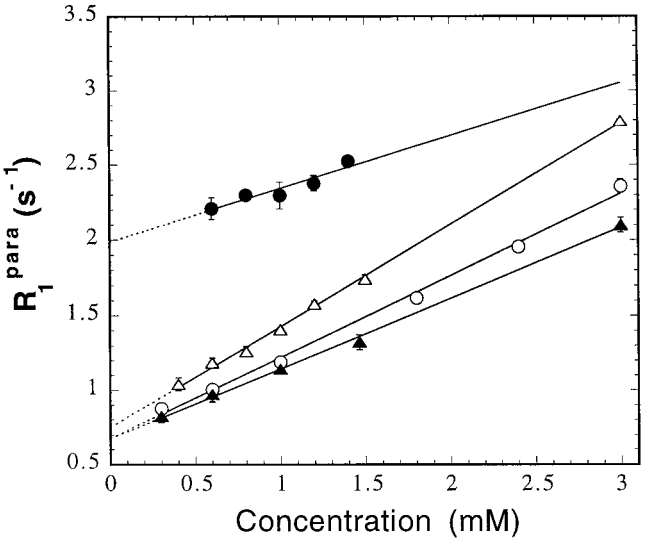

FIGURE 4 Spin-lattice relaxation rate at 500 MHz and 298 K for the tryptophan protons in spin-labeled peptides S1SL (Δ), S2SL (○), S3SL (▲), and H2SL (●) plotted as a function of peptide concentration.

The slopes and intercepts of the linear regression analysis are summarized in Table 2. As seen in Fig. 4 and Table 2, the slope of the concentration dependence of R_1^{SL} for the three linear peptides decreases with increasing peptide length. Also shown in Table 2 is the ^{13}C relaxation rate, R_1^{SL}, as a function of concentration for the ^{13}C labeled peptide, H2SL (the relaxation rate of the ^{13}C label in the C-terminal alanine was measured, because the ^{13}C label on the N-terminus was not observable in the presence of the spin label). The concentration dependence of the ^{13}C relaxation rate of this peptide is much weaker than the ^{1}H cases, which is consistent with the smaller ^{13}C magnetogyric ratio. The intercepts shown in Table 2 represent the intramolecular contribution to the relaxation rates, R_1^{para}. The relaxation rate for the non-spin-labeled version of the identical peptide R_1^{dia} (see Table 2) was then subtracted from this rate (Eq. 1) to obtain the paramagnetic contribution to the relaxation rate, R_1^{enh}. The paramagnetic contribution to the observed tryptophan proton relaxation rate for the linear peptides ranged between 12% for the longest peptide and 33% for the shortest Peptide.

Table 3 summarizes the intermoment distances calculated from the paramagnetic enhancement and the correlation times. As expected, the measured distance between the nitroxide and the tryptophan aromatic protons increases with increasing spacer length. The peptides that incorporate

TABLE 2 Relaxation rates obtained from the concentration dependence of R_1^{SL}

Peptide	Slope (s^{-1} mol^{-1})	Intercept R_1^{para} (s^{-1})	R_1^{dia} (s^{-1})	R_1^{enh} (s^{-1})
S1	0.677 ± 0.013	0.749 ± 0.019	0.560 ± 0.009	0.190 ± 0.021
S2	0.545 ± 0.018	0.674 ± 0.032	0.547 ± 0.001	0.127 ± 0.01
S3	0.470 ± 0.013	0.672 ± 0.020	0.598 ± 0.006	0.074 ± 0.021
H1	0.380 ± 0.073	2.005 ± 0.076	0.575 ± 0.019	1.430 ± 0.078
H2	0.014 ± 0.002	0.820 ± 0.011	0.393 ± 0.032	0.427 ± 0.034

The errors shown are standard errors. The slope and intercept (R_1^{para}) are obtained from a linear fit to the concentration dependence of R_1^{SL} (see Fig. 4) using the spin-labeled version of the indicated peptide. The slope provides a measure of the contributions made by intermolecular electron–nuclear interactions to the nuclear relaxation rate. R_1^{dia} is the relaxation rate of the non-spin-labeled version of the peptide, and R_1^{enh} is the intramolecular paramagnetic enhancement determined from Eq. 1.

a glycine hinge, H1 and H2, exhibited large paramagnetic enhancements; H1SL and H2SL demonstrated four-fold and two-fold increases, compared to the relaxation rates of the respective unlabeled peptides. The electron–nuclear distances estimated from the paramagnetic enhancements in these hinged peptides (see Table 3) are 19 Å shorter than that expected for a comparable linear peptide.

The dependence of intermoment distance on peptide length in the S1–S3 series is qualitatively reasonable, but the effective length increase per proline residue is only 1.1 to 1.7 Å. This result is far less than the expected average distance of 3.4 Å per proline residue in a type II helix. The distances between the nitroxide and the proton at position 4 of the indole ring of tryptophan were determined from linear molecular models of the peptides S1–S3 and the distances summarized in Table 3. The experimental distances are considerably shorter than these distances and, for S3, are approximately 7 Å shorter than expected.

One cause for the differences between the distances obtained from the relaxation rates and the rigid models may be internal molecular motions. Although we do not have any knowledge of molecular trajectories that may provide accurate calculations of $\langle r^{-3}\rangle^2$, we examined molecular dynamics simulations of S1–S3 and computed a 100-ps average of $\langle r^{-3}\rangle^2$, and the results are summarized in Table 3. In these simulations, the proline helix remained relatively rigid, consistent with previous work indicating that the poly-proline type II helix is rigid (Stryer and Haugland, 1967). Much of the variation in the electron–nuclear distance appeared to arise from flexibility in the spin-label linkage and the position of the tryptophan side chain. As expected, the distances obtained from these simulations are shorter than those obtained from the linear rigid peptide models, and the increase in distance as the proline linker is lengthened is close to the expected distance for proline in a type II helix.

Modeling the relaxation rates.

A second potential source of distance error may be a failure of the approximation that the electron–nuclear dipole–dipole coupling dominates all others. At short electron–nuclear distances, this is an excellent approximation. At long distances the approximation fails when proton–proton relaxation rates are comparable to the long range direct electron–nuclear coupling. If neighboring protons are not equidistant from the paramagnetic center, the proton relaxation rates will be different and neighboring protons will have different spin temperatures. As a consequence the relaxation rate of the spin most distant from the electron spin may be enhanced indirectly, and the distance deduced shorter. To determine whether this is likely to be a significant effect in these systems, a relaxation simulation was performed on the peptide S1SL.

Beginning with the peptide S1SL in an energy-minimized type II poly-proline helix, a relaxation matrix was constructed, which included the 63 protons in this structure and one electron. This matrix included all possible pairwise

TABLE 3 Comparison of intermoment distances from experiment and molecular modeling

Peptide	τ_c (ns)*	Distance (Å)*	Limits (Å)		Distance (Å)§ (static linear model)	MD Distance (Å)§ $(1/b)^{1/6}$
			Lower	Upper		
S1	0.83	18.6	18.3	19.0	21.7	17.1
S2	0.89	19.7	19.5	20.0	23.7	21.5
S3	0.95	21.4	20.5	22.6	28.3	24.0
H1	0.92	13.1	13.0	13.2	29.3	10.2
H2	0.92	14.1	14.3	14.5	—	—
H2	0.19	11.3	11.1	11.4	—	—

*The correlation times were calculated using Eq. 3 and intermoment distances from Eq. 2. The distance bounds listed here were calculated based on the standard errors in the relaxation enhancement given in Table 2.

§Distances for the static linear model were obtained by building type II proline helices and measuring distances for energy-minimized structures. The weighted distance is given as $(1/b)^{1/6}$, where $b = \langle r^{-3}\rangle^2$. The simulations were carried out for a duration of 100 ps at a temperature of 300 K.

interactions between protons or between protons and the electron with the appropriate interspin distances. In this model each spin was assumed to have an identical correlation time equal to the overall tumbling rate of the molecule (~0.95 ns). This relaxation matrix, which represents the coefficients of 64 coupled differential equations, was solved using numerical methods as described above (see Methods), and the results are shown in Fig. 5. The normalized magnetization decays shown in Fig. 5 indicate that relaxation rate of the observed proton in the presence of the spin label is enhanced slightly by the presence of nearby interacting protons. Under the set of conditions shown here, the paramagnetic enhancement is altered by about 30%. As a result, Eq. 2 will underestimate the actual distance because the contributions due to neighboring interacting protons have been ignored. However, this effect is small and the error introduced by this approximation results in a shortening of the electron–nuclear distance by about 0.8 Å, or by about 5% for the simulation shown in Fig. 5. Although this may make a proportionally larger contribution at larger distances, it is not large enough to account for the differences between the measured and predicted distances shown in Table 3.

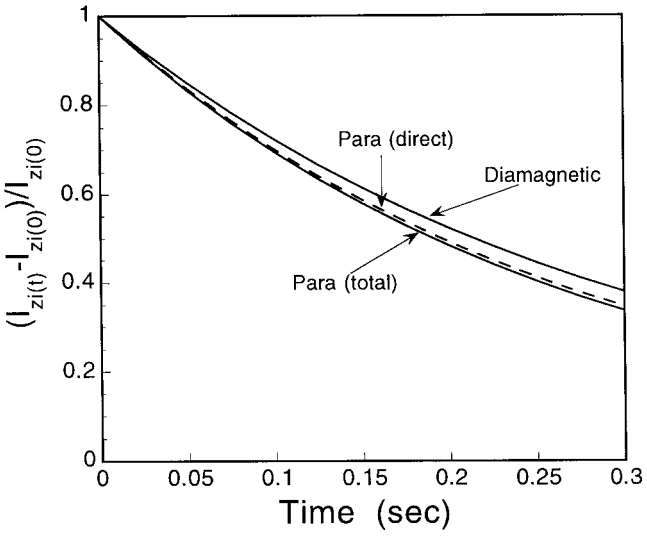

FIGURE 5 Calculated magnetization decay for the system of 63 protons in the linear conformation predicted for the peptide (S1SL). The rotational correlation time was assumed to be uniform throughout the peptide and was taken to be 0.95 ns. The predicted magnetization decay for the H-4 indole in tryptophan is shown with and without the attached spin label on the N-terminus. The solid lines are calculated using both diagonal (direct) and off diagonal (cross-relaxation) terms. The dotted lines represent the rates that are predicted with the cross-relaxation rates set to zero. Cross-relaxation rates make significant contributions to both the diamagnetic and paramagnetic experiments. However, the determination of distance made using Eqs. 1 and 2 assumes an interaction between an isolated proton and electron, and it does not take into account the contribution made by cross-relaxation among protons, which may develop different spin temperatures because of different distances to the paramagnetic center.

DISCUSSION

In the data presented above, paramagnetic enhancements of proton relaxation were examined in a series of model poly-proline helices to estimate time-averaged intramolecular distances. When linear and hinged peptides are compared, the larger relaxation enhancements for the flexible peptides demonstrate clearly that molecular flexibility is easily sensed by this NMR distance measurement. However, the distance average is complex and only approximated molecular dynamics simulations that cover a relatively short time scale.

An important observation from these data is that, even in the linear poly-proline helices, the intermoment distances were shorter than expected based on linear rigid structures; however, distances based on molecular dynamics trajectories of these peptides did a better job of approximating the experimental distances. This result is in contrast to classic fluorescence studies on similar poly-proline type II helices, where a close match with the expected lengths of these helices was found (Stryer and Haugland, 1967). It is crucial to note that, although both fluorescence energy transfer and nuclear spin-lattice relaxation enhancements depend on dipole–dipole interactions in the same way, the time period over which the interactions are averaged are dramatically different. The nuclear spin-lattice relaxation times are on the order of a tenth of a second or longer and thus report distances averaged over this period. Fluorescence energy transfer is limited by fluorescence lifetimes, which are seven or eight orders of magnitude shorter than the nuclear spin-lattice relaxation times. Indeed, in highly flexible systems, fluorescence energy transfer appears to provide information on distance distributions in macromolecules rather than information on time average distances (Hochstrasser et al., 1992).

For the linear peptides S1–S3, the measured distances are substantially less than that predicted based on linear models. The molecular dynamics simulation suggests the reason. However, the failure of the dynamics simulations to reproduce the measured distances accurately is expected because the simulation runs for such a short time. These simulations cover a relatively short time scale (100 ps), whereas the NMR relaxation measurement intergrates over a period of milliseconds to seconds. As a result, setting aside other criticisms of the simulation approach, the simulation is unlikely to sample the same range of intermoment distances and trajectories as those yielding the experimental data.

As indicated above, our use of the Solomon–Bloombergen equation assumes that paramagnetic enhancements result entirely from a direct interaction between the free electron and the observed nucleus. The computational results shown in Fig. 5 address the possible indirect effects of the paramagnetic center. However, the electron–nuclear distances in these molecules are not long enough that proton mediated paramagnetic contributions may dominate. It should be noted that our use of the Solomon–Bloombergen equation also assumes a single correlation time. In fact, an

anisotropic model that includes both perpendicular and parallel rates would be more appropriate for the rod-like molecules examined here. However, the effects of anisotropic motion will be small and will tend to slightly decrease the distance estimate. Thus, this assumption cannot account for the shorter than expected distances noted in Table 3. As indicated above, the distance estimate is relatively insensitive to the apparent correlation time because it only depends upon the sixth root of τ_c, and in fact, altering τ_c by a factor of 4 alters the distance estimate by less than 1 Å.

These results are similar to earlier work using paramagnetic enhancements to investigate molecular fluctuations in the peptide alamethicin. In this case it was clear that end-to-end distances are much shorter than expected based on the crystal structure (North et al., 1994). Most earlier distance measurements using paramagnetic enhancements in proteins have not been applied to probe internal molecular dynamics. For example, Schmidt and Kuntz used line-broadening produced by a spin label to determine the position of the spin-labeled site in lysozyme (Schmidt and Kuntz, 1984), and spin labels have been used to determine the solvent exposure of nuclei in macromolecules (Fesik et al., 1991). As demonstrated here, distance measurements based on paramagnetic enhancements of nuclear spin-lattice relaxation should provide a useful dynamical probe. Because of the strong weighting of short distances in the time average, the distances extracted will generally be near the distance of closest approach.

In summary, a series of peptides based on poly-L-proline were synthesized with a spin label at the N-terminus and used to investigate the effect of spacing on the magnitude of the electron–nuclear dipolar interaction sensed by resonances at a C-terminal tryptophan. The experimental distances are shorter than those expected based on rigid helical models because the NMR relaxation time measures a time-averaged weighted distance. When a highly flexible spacer is placed in the central portion of a poly-L-proline peptide, the peptide end-to-end distance sensed by the dipolar coupling decreases dramatically, demonstrating that these measurements are sensitive to the flexibility of the macromolecule being investigated. This class of measurement should facilitate the investigation of both local and large-scale structural fluctuations in proteins and other macromolecules, particularly when combined with high-resolution structural information from crystallography.

This research was supported by grants from the National Institutes of Health, GM-35215 to DSC and GM-34541 to RGB.

REFERENCES

Bloombergen, N., E. M. Purcell, and R. V. Pound. 1948. Relaxation effects in nuclear magnetic resonance absorption. *Phys. Rev.* 73:679–712.

Cavanagh, J., W. J. Fairbrother, A. G. Palmer, and N. J. Skelton. 1996. Protein NMR Spectroscopy: Principles and Practice. Academic Press, Inc., San Diego, CA.

Fesik, S. W., G. Gemmecker, E. T. Olejniczak, and A. M. Petros. 1991. Identification of solvent-exposed regions of enzyme-bound ligands by nuclear magnetic resonance. *J. Am. Chem. Soc.* 113:7080–7081.

Hochstrasser, R. A., S. M. Chen, and D. P. Millar. 1992. Distance distribution in a dye-linked oligonuleotide determined by time-resolved fluorescence energy transfer. *Biophys. Chem.* 45:133–141.

Isied, S. S., and A. Vassilian. 1984. Electron transfer across polypeptides. *J. Am. Chem. Soc.* 106:1726–1736.

Krugh, T. R. 1976. Spin-label-induced nuclear magnetic resonance relaxation studies of enzymes. *In* Spin Labeling, Theory and Applications. Academic Press, New York. 339–372.

Lee, Y.-H., B. L. Currie, and M. E. Johnson. 1986. Interaction of spin-labeled phenylalanine analogue with normal and sickle hemoglobins: detection of site-specific interactions through spin-label-induced 1H NMR relaxation. *Biochemistry.* 25:5647–5654.

North, C. L., C. J. Franklin, R. G. Bryant, and D. S. Cafiso. 1994. Molecular flexibility demonstrated by paramagnetic enhancements of nuclear relaxation. Application to alamethicin: a voltage-gated peptide channel. *Biophys. J.* 67:1861–1866.

Rosevear, P. R., D. C. Fry, A. S. Mildvan, M. Doughty, C. O'Brian, and E. T. Kaiser. 1984. NMR studies of the backbone protons and secondary structure of pentapeptide and heptapeptide substrates bound to bovine heart protein kinase. *Biochemistry.* 23:3161–3173.

Schmidt, P. G., and I. D. Kuntz. 1984. Distance measurements in spin-labeled lysozyme. *Biochemistry.* 23:4261–4266.

Solomon, I. 1955. Relaxation processes in a system of two spins. *Phys. Rev.* 99:559–565.

Sternlicht, H., and E. Wheeler. 1967. Preliminary magnetic resonance studies of spin labeled macromolecules. *In* Magnetic Resonance in Biological Systems. Pergamon, Oxford, U.K. 325–334.

Stryer, L. 1978. Fluorescence energy transfer as a spectroscopic ruler. *Ann. Rev. Biochem.* 47:819–846.

Stryer, L., and R. P. Haugland. 1967. Energy transfer: a spectroscopic ruler. *Proc. Natl. Acad. Sci. USA.* 58:719–726.

Stewart, J. M., and J. D. Young. 1984. Solid Phase Peptide Synthesis. Pierce Chemical Co., Rockford, IL.